agronomy

Review

The Increase in the Karstification–Photosynthesis Coupled Carbon Sink and Its Implication for Carbon Neutrality

Yanyou Wu [1,*] and Yansheng Wu [1,2]

1 State Key Laboratory of Environmental Geochemistry, Institute of Geochemistry, Chinese Academy of Sciences, Guiyang 550081, China
2 University of Chinese Academy of Sciences, 100049 Beijing, China
* Correspondence: wuyanyou@mail.gyig.ac.cn

Abstract: Two of the most important CO_2 sequestration processes on Earth are plant photosynthesis and rock chemical dissolution. Photosynthesis is undoubtedly the most important biochemical reaction and carbon sink processes on Earth. Karst geological action does not produce net carbon sinks. Photosynthesis and karstification in nature are coupled. Karstification–photosynthesis coupling can stabilize and increase the capacity of karstic and photosynthetic carbon sinks. Bidirectional isotope tracer culture technology can quantify the utilization of different inorganic carbon sources by plants. Bicarbonate utilization by plants is a driver of karstification–photosynthesis coupling, which depends on plant species and the environment. Carbonic anhydrase, as a pivot of karstification–photosynthesis coupling, can promote inorganic carbon assimilation in plants and the dissolution of carbonate rocks. Karst-adaptable plants can efficiently promote root-derived bicarbonate and atmospheric carbon dioxide use by plants, finally achieving the conjugate promotion of karstic carbon sinks and photosynthetic carbon sinks. Strengthening karstification–photosynthesis coupling and developing karst-adaptable plants will greatly improve the capacity of carbon sinks in karst ecosystems and better serve the "Carbon peak and Carbon neutralization" goals of China.

Keywords: bicarbonate use; carbon sequestration; carbonic anhydrase; karst; karst-adaptable plants; photosynthesis

check for updates

Citation: Wu, Y.; Wu, Y. The Increase in the Karstification–Photosynthesis Coupled Carbon Sink and Its Implication for Carbon Neutrality. *Agronomy* **2022**, *12*, 2147. https://doi.org/10.3390/agronomy12092147

Academic Editor: Arnd Jürgen Kuhn

Received: 10 August 2022
Accepted: 6 September 2022
Published: 9 September 2022

1. Introduction

Since the Industrial Revolution, atmospheric carbon dioxide (CO_2) concentrations have increased from 280 ppm before the Industrial Revolution to 421 ppm today, an increase of 50% [1]. Since 1850–1900, the global average surface temperature has risen by approximately 1 °C with the increase in atmospheric CO_2 concentrations [2]. Human activities have become one of the driving forces of changes in the Earth system, alongside the sun and the Earth's core, and the resulting global warming phenomenon has become a topic of major public concern. The impact of this phenomenon on the environment in which human beings live has become more direct. To prevent the occurrence of global warming, it is urgent to carry out research into effective and economical atmospheric carbon dioxide capture (carbon sequestration) pathways and take corresponding countermeasures. For this reason, China has made a commitment to reach carbon peak in 2030 and carbon neutrality in 2060, and to fulfill its responsibilities for the realization of global governance and the construction of a community with a shared future for humankind.

Karst is a general term for the geological effects of water on soluble rocks via mainly chemical dissolution, supplemented by mechanical actions such as erosion, latent erosion, and the collapse of flowing water, and the general term for the phenomena produced by these effects [3]. The global karst distribution area is nearly 22 million km^2, accounting for approximately 15% of the planet's land area, and the population living on karst areas is approximately one billion and is mainly concentrated in low latitudes, including Southwest

China, Southeast Asia, Central Asia, the Mediterranean, the east coast of North America, the Caribbean, the west coast of South America, and the south of Australia. Concentrated contiguous karst is mainly distributed in southern Europe, eastern North America and southwestern China. Karst in Southwest China is known for its larger continuous distribution area and for being the complete development type, the beautiful landscape and the fragile ecological environment [4,5]. In the 1,071,400 km^2 geographical range of 451 counties (cities) of Yunnan, Guizhou, Guangxi, Hunan, Guangdong, Sichuan, Chongqing, Hubei, and other provinces (autonomous regions and cities) centered on the Yunnan-Guizhou Plateau, the distribution area of carbonate rock is 450,800 km^2, accounting for 42.08% of the total land area [6].

Two of the most important processes for absorbing carbon dioxide on Earth are the photosynthesis of plants (biological action) and the chemical dissolution of rocks (silicate and carbonate rocks) (geological action). Photosynthesis is undoubtedly the most important biochemical reaction and carbon sink process on Earth. Plants use sunlight energy through photosynthesis to assimilate inorganic carbon and water into organic matter, release oxygen, couple the water and carbon metabolism of plants, and connect the soil–vegetation and vegetation–atmosphere systems. The equation for the dissolution of silicate rocks is as follows: $CO_2 + Ca(Mg)SiO_3 \rightarrow Ca(Mg)CO_3 + SiO_2$, and that for the dissolution of carbonate rocks (karstification) is as follows: $Ca(Mg)CO_3 + H_2O + CO_2 \rightleftarrows Ca(Mg)^{2+} + 2HCO_3{}^-$. The dissolution of silicate rocks is also undoubtedly a geological carbon sink process, but due to the low dissolution rate of silicate rocks [7], it is believed that silicate rock dissolution is only a carbon sink on a billion-year geological time scale [8], and has little impact on the carbon sink of the short-term time scale that human society is currently concerned about.

The dissolution of carbonate rocks has a profound effect on carbon sinks on short time scales [9–13]. From a short time scale, the development and utilization of fossil fuels released a large amount of carbon dioxide in advance due to human activities, especially the industrial revolution, which breaks the balance between the sequestration of carbon dioxide and the release of carbon dioxide, and conversely affects carbonate rock dissolution. Meanwhile, the lag in plant development and evolution has led to insufficient photosynthetic carbon sequestration. Therefore, the effect of carbonate rocks dissolution on carbon sinks is more profound on a short time scale.

Karstification by itself is a zero-carbon sink geological process, due to the balance of dissolution and the deposition of carbonate rocks on a billion-year-long time scale. Based on the models constructed from the deposition and burial of carbonates and organics, and the continental weathering of silicates, carbonates, and organics, as well as other factors such as volcanoes, diagenesis, and metamorphic degassing, scientists have found that after entering the ocean, $HCO_3{}^-$ dissolved from carbonate will be transformed into carbonates in seafloor sedimentary rocks while releasing CO_2. From the geological process of carbonate dissolution on land to marine sedimentation, karst geological action does not produce net carbon sinks [14–16].

2. Uncoupled Karstification Limits Photosynthetic Carbon Sequestration

2.1. Karst Drought

Drought is mostly caused by low precipitation, while karst drought are mainly caused by special geological environments, because the average annual rainfall in the karst region of Southwest China is sufficient, up to 1000~1800 mm [17]. Long-term strong karstification has caused the hydrogeological structure in karst areas to be a special spatial structure on the surface and underground. The underground river system in this area is very well developed, and the surface has developed a large number of karst landforms in different landscapes, such as caves, lysophores, lysses, funnels and sinkholes, and skylights. Because most of the rocks are exposed and soil formation is slow and the soil layer is shallow, rainwater quickly leaks into the ground, becoming deeply buried groundwater, forming a pattern of separation between water and soil, and the water covered by the thin soil is quickly evaporated, resulting in soil drought [18]. When torrential rains fall, the underground karst pipes do not provide sufficient drainage, resulting in flooding [19,20]. Karst drought causes the stomata of leaves to close, severely reducing the photosynthesis of plants, and it even causes the death of plants.

2.2. High pH, and High Bicarbonate and Calcium Contents

Most of the bedrock in karst habitats consists of carbonate rocks, and its main chemical components are soluble salts such as $CaCO_3$ and $MgCO_3$. Due to the continuous dissolution of carbonate rocks in these habitats, hydrogen ions were consumed, a large number of bicarbonate ions and calcium and magnesium ions were formed, and the cover soil was modified into an environment with a high pH and high content of calcium and bicarbonate that affected the nutrient uptake by plants [18,21–23].

The average pH of the soil in the karst area of Mulun National Nature Reserve was 6.96, the maximum value was 7.68, and the minimum value reached 5.76 [24]. The pH of the soil developed from limestone was 7.69, and that from dolomite was 7.85, which was significantly higher than that from shale (5.32), sandstone (5.44), and red clay (5.32) [25].

The average exchangeable calcium content in the soil of Puding, Huajiang, Libo, and Luodian in karst areas was 3612.43 $mg \cdot kg^{-1}$, which was seven times higher than the value of 519.33 $mg \cdot kg^{-1}$ found in the non-limestone soils of Fujian, and more than 250 times higher than the average of 14.22 $mg \cdot kg^{-1}$ in the non-limestone soils of hilly and mountainous regions in southern China [26–28].

2.3. Deficiency of Available Nitrogen, Phosphorus, and Nutrient Elements

In karst areas, due to strong dissolution, many effective nutrient elements in the soil are lost. In addition, the high pH value and calcium concentration of the soil further reduce the effective the content of nutrient elements.

Due to the high pH value and high concentration of bicarbonate in soils of karst areas, ammonium nitrogen easily generates ammonia and enters the atmosphere [29]. Therefore, the content of ammonium nitrogen in karst areas is often lower than that in nonkarst areas, while the content of nitrate nitrogen is often higher than that in nonkarst areas. The average content of ammonium nitrogen from 20 soil samples in karst areas was 5.09 $mg \cdot kg^{-1}$, which is less than 70% of that of the Loess Plateau, while the average content of nitrate nitrogen was 13.60 $mg \cdot kg^{-1}$, which is 6.5 times that of the Loess Plateau [30,31]. A low content of ammonium nitrogen and a high content of nitrate nitrogen are typical characteristics of soil in karst areas.

The high pH value and calcium of soil in karst areas make it difficult for phosphorus and other nutrient elements in soil to move, resulting in a lack of available phosphorus and nutrient elements. The average value of available phosphorus in the soil in the limestone area was only 1/3 of that in the sandstone area [31]. The contents of available Zn, Cu, and B in calcareous soil in Guangxi were 1.48, 1.45, and 0.04 mg kg^{-1}, respectively [32], while the contents of available Zn, Cu, and B in the topsoil of paddy soil measured in Yixing city, Jiangsu Province, in 1995 were 3.94, 5.12, and 0.28 mg kg^{-1}, respectively [33]. Clearly, the contents of available Zn, Cu, and B in calcareous soil in Guangxi Province are significantly lower than those in paddy soil in Yixing city, Jiangsu Province.

Therefore, deficiencies in available nitrogen, phosphorus, and other nutrients in karst areas, which limit plant growth and development, are another limiting factor for plant photosynthetic carbon sequestration in karst areas.

3. Karstification–Photosynthesis Coupling Increases Karst Carbon Sinks

Plants (including microalgae) not only directly use carbon dioxide from the atmosphere, but also bicarbonate from soil (water bodies) [34–40], which transform bicarbonates from karstification into photosynthetic carbon sinks [35,41]. Both photosynthetic organisms in the ocean (or other water bodies) and terrestrial plants can "intercept" partial bicarbonate to form a photosynthetic carbon sink. Some bicarbonate dissolved from carbonate becomes sedimentary rock on the seafloor; however, a considerable amount of bicarbonate is involved in photosynthetic assimilation into organic matter. Aquatic photosynthetic organisms and terrestrial plants "intercept" inorganic carbon, which is then replenished with atmospheric CO_2 to capture it. Therefore, the "interception" of bicarbonate by plants stabilizes the apparent karst carbon sink, results in the coupling of karstification and photosynthesis, and yields a net karst carbon sink.

In fact, photosynthesis and karstification in nature are coupled (Figure 1) [42–45]. Karstification–photosynthesis coupling has always constrained atmospheric CO_2 concentrations. In geological history, higher concentrations of atmospheric CO_2 occurred in periods of lagging photosynthesis development, high CO_2 levels in the early Paleozoic era were associated with non-land plant continents, and low CO_2 levels in the Permian-Carboniferous period were associated with the occurrence, development, and flourishing of vascular plants [14,46–48]. Karstification–photosynthesis coupling connects the atmosphere, hydrosphere, and lithosphere through the biosphere, attenuating long-term CO_2 variability and resulting in the atmospheric composition remaining constant from pre-75 Ma to the Holocene (pre-Industrial Revolution) [49–54].

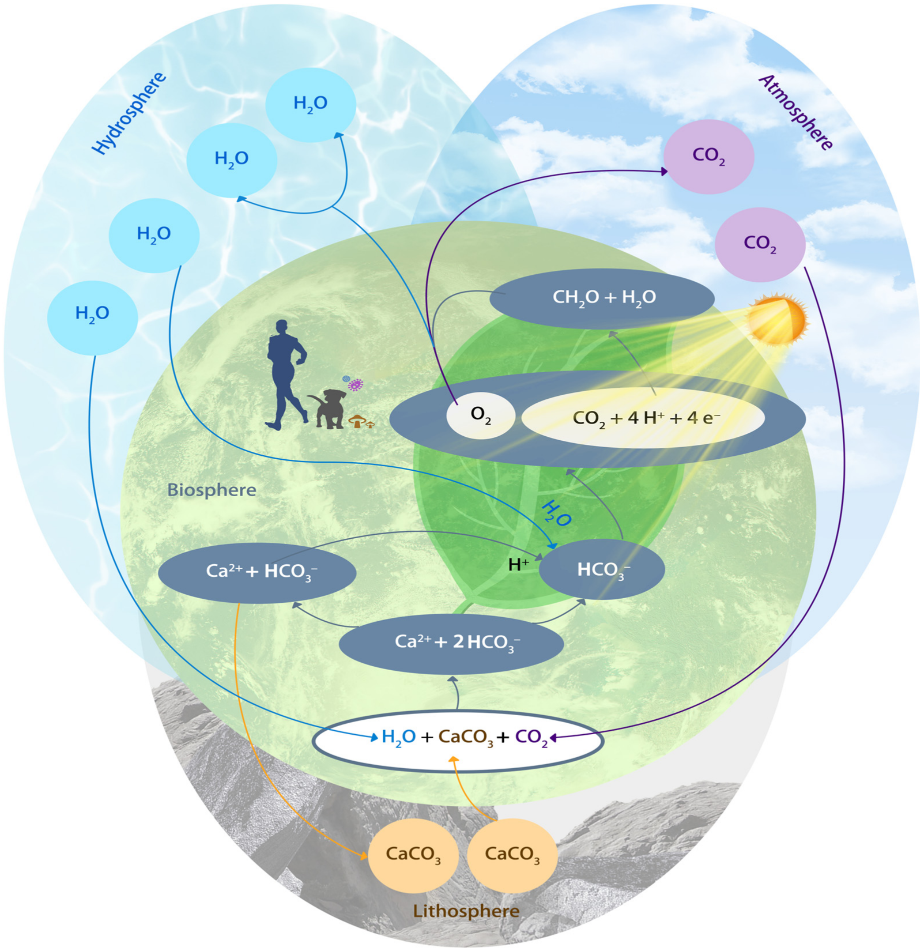

Figure 1. Karstification–photosynthesis coupling processes and their role in the water–carbon balance in nature. Carbonate rocks (lithosphere) are dissolved under the action of water (hydrosphere) and carbon dioxide (atmosphere) to form Ca^{2+} and bicarbonate (biosphere) (carbon sink process). Ca^{2+} combines with bicarbonate to precipitate calcium carbonate ($CaCO_3$) into the lithosphere (carbon source process). Plants split bicarbonate and water to release oxygen and carbon dioxide, then assimilate carbon dioxide to form carbohydrates (CH_2O) (biosphere) (carbon sink process). Finally, organisms utilize oxygen to decompose carbohydrates into carbon dioxide that enters the atmosphere, and water that enters the hydrosphere (carbon source process).

The direct determination of carbonate rock dissolution or changes in bicarbonate seems to reflect the ability of carbonate rock to capture CO_2. However, due to the high variability of carbonate rock dissolution and carbonate rock deposition, as well as the resulting high temporal and spatial heterogeneity of bicarbonate, the application of the carbonate-rock-tablet test, solute load method, and maximum potential dissolution method is limited [11]. Even if the dissolution amount of carbonate can be determined by the carbonate-rock-tablet test, this can only partially reflect the weathering of carbonate (apparent karst carbon sink). In addition, even if changes in the bicarbonate of karstic catchments can be determined via the solute load method or the maximum potential dissolution method, this only partially reflects the instantaneous apparent karst carbon sink capability. The ability of terrestrial and aquatic plants to "intercept" (assimilate) bicarbonates, i.e., net karst carbon sinks, is difficult to obtain using these methods. However, the amount of bicarbonate utilized by plants can represent the net karst carbon sink capacity due to karstification–photosynthesis coupling in nature (Figure 2).

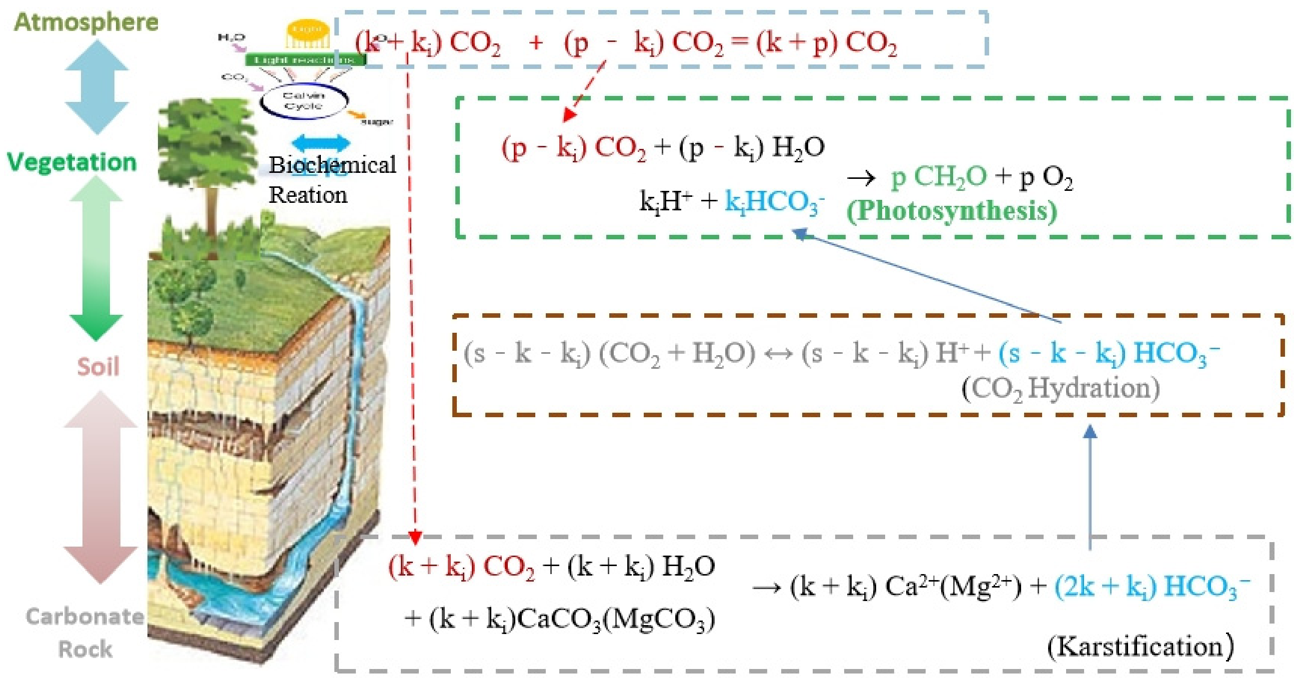

Figure 2. The determination principle of karstification, photosynthesis, and net karst carbon sink under karstification–photosynthesis coupling (example uses are terrestrial plants; aquatic plants replace soil with water bodies), where ki is the amount of root-originated HCO_3^- used by plants, k_i/p is the share of plant utilization of root-originated HCO_3^-, $k_i/(p - k_i)$ is the stoichiometric ratio of root-originated HCO_3^- and atmospheric CO_2 utilized by plants, p is the photosynthesis of plants, and $k + k_i$ is the karstification of carbonate rocks. It should be noted here that from the initial process of carbon sequestration, $p - k_i$ is the photosynthetic carbon sink of plants, $k + k_i$ is the apparent karst carbon sink of carbonate rocks, s is the carbon sink of soil, and $(k + k_i)/(p - k_i)$ is the stoichiometric ratio of karstification and photosynthesis under karstification–photosynthesis coupling. From the substantial process of carbon sequestration, p is the photosynthetic carbon sink of plants, which includes the direct carbon sink $p - k_i$ and the indirect carbon sink k_i, $k + k_i$ is the apparent karst carbon sink of carbonate rock, which includes the apparent karst basic carbon sink k and the intermediate carbon sink k_i from karstification–photosynthesis coupling, and k/p is the stoichiometric ratio of karstification and photosynthesis under karstification–photosynthesis coupling. It can also be seen that the karstification–photosynthesis coupling system not only increases the carbon sink of the system as a whole, but also increases the stability of the carbon sink in karst ecosystems, because the photosynthetic carbon sink is more stable than HCO_3^-.

Stable isotope techniques are widely used in tracing geological and biological processes [55]. Moreover, they can also successfully identify the role of plant photosynthesis, respiration, and water metabolism, and have become an important tool for studying the relationship between water and carbon in ecosystems [56–60]. However, due to the continuous conversion of various inorganic carbons and the continuous exchange of isotopes, conventional stable isotope technology is difficult to trace, and it is more difficult to quantify the utilization information of specific inorganic carbon sources. Therefore, to solve the problem of signal interference during inorganic carbon conversion and isotope exchange, we successfully developed a bidirectional isotope tracer culture technology. Bidirectional isotope tracer culture technology is used to simultaneously label and culture two identical plants with two kinds of bicarbonates at different stable carbon isotope ratios (the difference being more than 10‰), respectively, eliminate signal interference in the process of inorganic carbon transformation and isotope exchange by using parallel isotope difference signals, and finally, analyze and quantify the utilization information of different inorganic carbon sources. Now, bidirectional isotope tracer culture technology has become a promising technique for analyzing and quantifying the utilization of different inorganic carbon sources. Using this technique, combined with metabolic regulation technology (such as applying specific inhibitors), bicarbonate and CO_2 utilization by plants were quantified [34,36–38,40,41]. This technique was even used to successfully quantify the karstification and photosynthesis of microalgae [35,39,61]. Therefore, by comprehensively applying bidirectional isotope tracer culture technology, metabolic regulation technology, and physiological biochemistry, the stoichiometric relationship between karstification and photosynthesis, and HCO_3^- and CO_2 utilization by plants under karstification–photosynthesis coupling can be accurately quantified.

Bicarbonate utilization depends on the plant species and the environment. Isotopic techniques can be used to obtain the share of bicarbonate utilization by plants, and many studies have confirmed that karst-adaptable plants cope with karst adversity by increasing the share of bicarbonate utilization. The effect of sodium bicarbonate (10 mM) on photosynthetic carbon metabolism in karst-adaptable plants (*Broussonetia papyrifera*) using bidirectional isotope tracing culture techniques was studied [34]. The results showed that after 20 days of sodium bicarbonate treatment, the total photosynthetic rate of *Broussonetia papyrifera* was 2.65 μmol(CO_2) $m^{-2}{\cdot}s^{-1}$, of which the share of bicarbonate utilization accounted for 30%, while the total photosynthetic rate of mulberry trees (*Morus alba*) was 2.55 μmol(CO_2) $m^{-2}{\cdot}s^{-1}$, of which the utilization share of bicarbonate ions accounted for 0. Hang and Wu (2016) quantified the effects of different concentrations of sodium bicarbonate on photosynthetic carbon metabolism in the karst-adaptable plant *Orychophragmus violaceus*, using bidirectional isotope tracing culture techniques. The results showed that when concentrations of bicarbonate were 5, 10, and 15 mM, the share of bicarbonate utilization to the total carbon assimilation in *Orychophragmus violaceus* was 5.4%, 13.5%, and 18.8%, respectively. The bicarbonate utilization of *Brassica juncea* accounts for less than 5% of the total carbon assimilation [36].

When using polyethylene glycol 6000 (PEG 6000) to simulate karst drought to study the inorganic carbon assimilation response of *Orychophragmus violaceus* and *Brassica juncea* to PEG 6000, it was found that when the concentrations of PEG 6000 were 0, 10, 20, and 40 $g{\cdot}L^{-1}$, the shares of bicarbonate utilization to the total carbon assimilation of *Orychophragmus violaceus* were 6.7%, 13.1%, 17.6%, and 47.7%, respectively, and those of *Brassica juncea* were 2.9%, 7.6%, 7.7%, and 5.9%, respectively [62]. When the concentrations of PEG 6000 were 0, 100, and 200 $g{\cdot}L^{-1}$, the shares of bicarbonate utilization to the total carbon assimilation of *Camptotheca acuminata* were 10.34%, 20.05%, and 16.60%, respectively [37]. Under a simulated karst environment, after the 180-day growth phase, the shares of bicarbonate utilization to the total carbon assimilation of *Orychophragmus violaceus*, *Brassica juncea*, and *Euphorbia lathyris* were 11.45%, 10.39%, and 9.44%, respectively [38].

The degree of karstification–photosynthesis coupling and the net karst carbon sink capacity of ecosystems varies depending on land use. Table 1 shows the rate of dissolution measured via the carbonate-rock-tablet test method for different land use types. Table 2 shows carbon sink fluxes measured via the solute load method from several different karst catchments.

Table 1. Dissolution of different land use types.

Land Use	Average Dissolution Rate mg cm^{-2} y^{-1}	Karst Carbon Sink Intensity tCO_2 km^{-2} y^{-1}	Depth of the Underlying Carbonate-Rock-Tablet cm	Reference
Woodland	1.01	4.69	10	[63]
Dry land	4.25	19.72	60	
Paddy land	0.14	0.65	46	
Shrub	0.61	2.83	50	[64]
Dry land	5.27	24.45	50	
Paddy land	3.05	14.15	50	
Woodland	7.61	35.31	50	[65]
Grassland	8.89	41.25	50	
Vegetable-planted land	6.21	28.81	50	
Tilled land	11.0	51.04	20	[66]
Tilled land	14.9	69.14	50	
Shrub	0.5	2.32	20	
Shrub	2.6	12.06	50	
Woodland	68.7	318.77	20	
Woodland	18.7	86.77	50	
Orchard	87.7	406.93	20	
Orchard	120.1	557.26	50	

Table 2. Carbon sink fluxes (CSFs, tCO_2 km^{-2} y^{-1}) from several different karst catchments.

Catchment Name (Location)	CSFs	Reference	Catchment Name (Location)	CSFs	Reference
Banzhai (Libo)	28.84 ± 3.04	[67]	Huangzhou River (Shibing)	36.43	[68]
Huanghou (Libo)	32.81 ± 4.70		Chenqi (Puding)	55.07	[64]
Houzhai (Puding)	39.13 ± 7.56		Houzhai (Puding)	25.70	[69]

Dissolving 1 mol of carbonate rock can consume 1 mol of CO_2 from the atmosphere, contributing to the decline of atmospheric CO_2 concentration. Therefore, the rate of carbonate rock dissolution can reflect the karst carbon sink intensity. As seen from Table 1, the rate of dissolution varies depending on land use, different types of vegetation, or the same vegetation type for different observations. Karst carbon sink intensities range from 0.65 tCO_2 km^{-2} y^{-1} to 557.26 tCO_2 km^{-2} y^{-1}, with an average value of 98.60 tCO_2 km^{-2} y^{-1} and a median of 28.81 tCO_2 km^{-2} y^{-1}, which is only 2% of the average carbon sink capacity of karst forests (1447.05 tCO_2 km^{-2} y^{-1}) [70]. As seen from Table 2, carbon sink fluxes are different at different times and catchments, and even in the same catchments, with an average of 36.33 tCO_2 km^{-2} y^{-1} in the five catchments, which is only 2.5% of the average carbon sink capacity of karst forests [70]. Plants have a much greater ability to "intercept" (assimilate) bicarbonates than the karst carbon sink intensities measured via the carbonate-rock-tablet test method or carbon sink fluxes measured via the solute load method. For example, the average share of bicarbonate utilization by *Camptotheca acuminata* in July was 13.6%, and that in August was 18.8%. The average share of bicarbonate utilization by *Platycarya longipes* in July was 15.3%, and that in August was 14.3% [71]. It can be seen that net karst carbon sinks account for more than 80% of apparent karst carbon sinks.

The positive vegetation succession of the ecosystem represents an increase in karstification–photosynthesis coupling. Table 3 shows the distribution of net primary productivity and carbon sink capacity at various stages of karst vegetation succession in Maolan. Maolan karst vegetation is divided into five successional stages: herbaceous community, shrub–scrub community, shrub community, subclimax community of evergreen–deciduous broadleaved mixed forests, and climax community of evergreen–deciduous broadleaved mixed forests. The strongest karstification–photosynthesis coupling occurs in the climax community of evergreen–deciduous broadleaved mixed forests, and the weakest karstification–photosynthesis coupling occurs in herbaceous communities. The stronger the karstification–photosynthesis coupling between the plant community and carbonate rocks is, the greater the carbon sink in karst ecosystems [72].

Table 3. Distribution of net primary productivity (t hm^{-2} y^{-1}) and carbon sink capacity (tCO_2 km^{-2} y^{-1}) at various stages of karst vegetation succession in Maolan.

Succession Stage	Arbor Layer	Shrub Layer	Herbal Layer	Coarse, Medium Root	Fine Roots	Total	Carbon Sinks [1]
Climax community of evergreen-deciduous broadleaved mixed forests	7.01	0.25	0.04	1.51	4.72	13.58	2240.70
Sub-climax community of evergreen-deciduous broadleaved mixed forests	5.09	0.32	0.09	0.71	2.52	8.73	1440.45
Scrub–shrub community	1.39	0.79	0.06	0.57	3.27	6.08	1003.20
Herb–scrub community		1.03	0.60	0.85	2.10	4.58	755.70
Herb community			1.19	0.12	1.42	2.73	450.45

[1] Note: The conversion factor for converting plant net primary productivity into plant carbon sinks is 165.

4. Carbonic Anhydrase, a Key Pivot of Karstification–Photosynthesis Coupling

Carbonic anhydrase (CA, EC 4.2.1.1) specifically and efficiently catalyzes the reversible conversion of bicarbonate to CO_2 at 10^7 times the rate of the nonenzymatic reaction, being one of the fastest enzymatic reactions. CA is continuously distributed in the rock–soil interface and surface soil–vegetation ecosystems, and is widely present in various organisms in the soil, water, and rock surface layers [73–77]. Different organisms, and even the same organism, have different CA isoenzyme types and activities in different environments; therefore, CA has high heterogeneity [78–81]. Characterized by its continuous distribution, abundance, specificity, and efficient and rapid catalysis of the unique mutual conversion reaction between CO_2 and HCO_3^- in karst ecosystems, carbonic anhydrase is the only key biological enzyme that can closely couple karstification with photosynthesis, that is, inorganic and organic carbon between carbonate rocks–soil–vegetation–atmosphere. On the one hand, CA catalyzes the dissolution of carbonate rocks and the deposition of calcium carbonate to regulate karstification at the rock–soil interface. On the other hand, CA catalyzes the reversible conversion between carbon dioxide and bicarbonate in the soil solution and plants to regulate the photosynthesis and respiration of plants (Figure 3). Carbonic anhydrase is highly spatiotemporally heterogeneous and sensitive to the environment, and is dubbed the karstification "mortise", catalyzing the biogeochemical cycle of water–carbon, and even other elements, regulating the migration and transformation of substances between different interfaces, and maintaining the biodiversity and stability of the system [35,40].

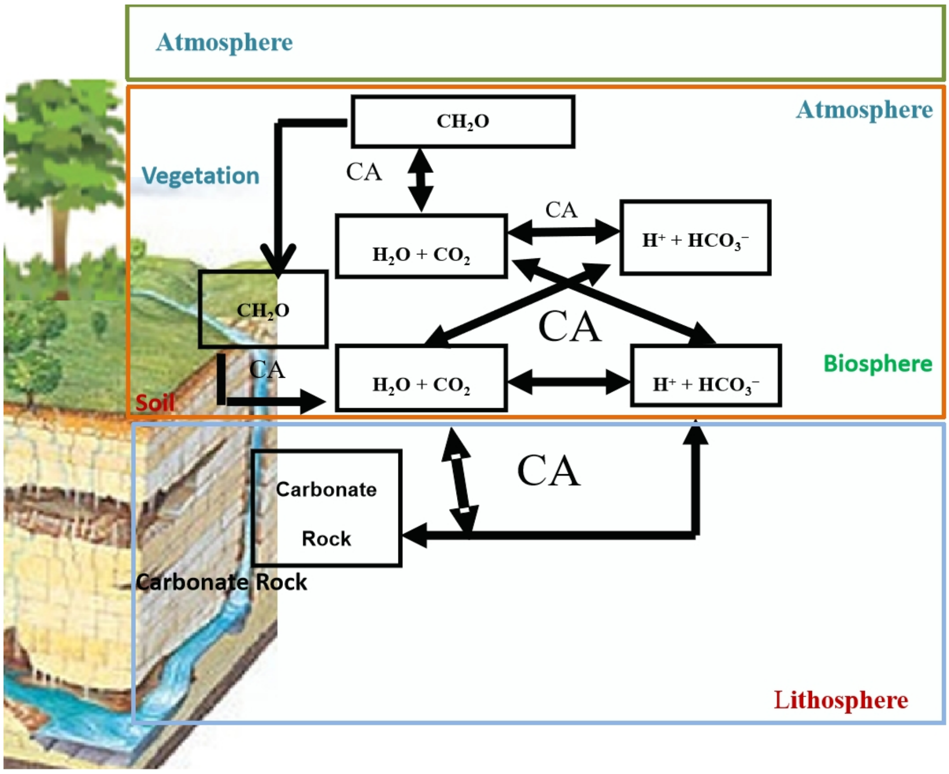

Figure 3. Carbonic anhydrase is pivotal in karstification–photosynthesis coupling. Carbonic anhydrase (CA) catalyzes the dissolution of carbonate rocks at the rock–soil interface, the hydration of CO_2 in the soil solution and soil–atmosphere and soil–vegetation interface, the photosynthesis of plants, etc.

4.1. Carbonic Anhydrase Controls the Transport of Water and Inorganic Carbon at the Carbonate Rocks–Soil–Atmosphere Interface by Catalyzing Carbonate Dissolution and Carbon Dioxide Hydration

The kinetically slow reaction $CO_2 + H_2O \leftrightarrow H^+ + HCO_3^-$ plays an important role in controlling the dissolution and precipitation of carbonate rocks in H_2O-CO_2-$CaCO_3$ systems [82]. Carbonic anhydrase, on the one hand, can quickly catalyze the CO_2 hydration reaction and improve the conversion rate between CO_2 and H^+ and HCO_3^-; on the other hand, the diffusion rate of related ions is affected by catalysis of the use of HCO_3^- and Ca^{2+} by organisms in the soil, thereby catalyzing the dissolution and sedimentation of carbonate rocks [83]. Exogenous CA, algal CA, and extracellular CA of microorganisms can promote the dissolution of carbonate rocks [61,83–85]. The flux of CO_2 in soil is also controlled by CA [86–88].

4.2. Carbonic Anhydrase Promotes Inorganic Carbon Assimilation in Plants

After plants experienced karst adversity, the stomatal conductivity was reduced or the stomata were closed, the atmospheric CO_2 supply was insufficient, and the absorption and transportation of water in roots were blocked. In response to water and CO_2 deficiencies, plants rapidly upregulated the gene expression of specific CA isoenzymes in leaves [40,89,90], increased the activity of corresponding CA isoenzymes [81,91], converted HCO_3^- from soil into water and CO_2, supplemented them to photosynthetic organs, improved the water supply and water efficiency, and increased the utilization of atmospheric CO_2 and HCO_3^- [34,36–38,40].

Carbonic anhydrase catalyzes the dissolution and sedimentation reaction of carbonate rocks at the rock–soil interface, which affects the concentration of HCO_3^- in soil controlled by the CA of plants and soil, and in turn affects the utilization of HCO_3^- by plants. Bicarbonate utilization not only provides plants with metabolic water (intracellular water), increases stomatal opening, and directly increases the assimilation of CO_2, but also increases the photosynthetic area by increasing the adaptability and promoting the growth of plants [40]. In addition, the concentration of bicarbonate in soil can also affect CO_2 fluxes in soil, which are also regulated by CA [77,92].

5. Carbon Sequestration and the Enhancement Effect of Karst-Adaptable Plants during Karstification–Photosynthesis Coupling

After the Industrial Revolution, buried fossil fuels were exploited in large quantities, releasing a large amount of carbon dioxide over a short time, while plant adaptive evolution and development lagged behind, resulting in karstification–photosynthesis decoupling, which eventually led to a global increase in carbon dioxide. After karstification–photosynthesis decoupling, karst-adaptable plants evolve gradually to adapt to karst environments of karst drought, high pH, and high contents of calcium and bicarbonate, and their unique adaptation mechanisms and strategies in turn can accelerate to reach a new degree of karstification–photosynthesis coupling [40,93,94].

Karst-adaptable plants efficiently use bicarbonate, compensatorily absorb nitrate nitrogen, and attain higher photosynthetic carbon sequestration capacity at a lower cost [95], thereby stimulating plant growth, increasing the photosynthetic area, and then promoting root-originated bicarbonate and atmospheric carbon dioxide use by plants, further enhancing photosynthetic carbon sinks. Moreover, karst-adaptable plants reduce the content of bicarbonate in rhizosphere soil during the use of bicarbonate. As a result, the dissolution effect of carbonate rock is further strengthened to supplement bicarbonate into the soil, which further promotes the karst carbon sink capacity, promotes root-originated bicarbonate use by plants, and finally achieves the conjugate promotion of karst carbon sinks and photosynthetic carbon sinks. In fact, karstification that is not coupled with photosynthesis has a limited carbon sink capacity, but if karstification has a high degree of coupling with photosynthesis, its carbon sink capacity is extremely huge. Theoretically, the carbon sink capacity of an 8-year woody plant with karstification–photosynthesis coupling of 10% will be twice that without karstification–photosynthesis coupling. The carbon sink capacity of a 10-year woody plant with a karstification–photosynthesis coupling of 10% is 1.6 times that with a karstification–photosynthesis coupling of 5% ($1.10^{10}/1.05^{10}$); thus, the karst carbon sink capacity is 3.2 times that of the latter.

6. Conclusions and Outlook

Karst geological action by itself is a zero-carbon sink process on a billion-year long time scale. Uncoupled karstification limits photosynthetic carbon sequestration by plants. Karstification–photosynthesis coupling, driven by the bicarbonate utilization of plants and pivoted by carbonic anhydrase, can promote inorganic carbon assimilation in plants and the dissolution of carbonate rocks, thereby stabilizing and increasing the capacity of karst carbon sinks and photosynthetic carbon sinks. Karstification–photosynthesis coupling determines the carbon sink of karst ecosystems. Full use of the adaptation strategies of karst-adaptable plants with high karstification–photosynthesis coupling can maximize carbon sequestration and the enhancement effect of plants in karst areas. Finally, a carbon sequestration system encompassing ecological restoration, rocky desertification control, and the sustainable use of plant resources can be developed.

Author Contributions: Y.W. (Yanyou Wu) and Y.W. (Yansheng Wu) cooperated to complete this article. All authors have read and agreed to the published version of the manuscript.

Funding: This work was supported by the National Natural Science Foundation of China (No. U1612441-2) and Support Plan Projects of Science and Technology of Guizhou Province (No. (2021)YB453).

Institutional Review Board Statement: Not applicable.

Data Availability Statement: All data generated or analyzed during this study are included in this published article.

Acknowledgments: We deeply thank K. Murali, C. Zeng, X. Bai, and Z. Liu for valuable comments. I am grateful to M. Wu for help with Figure 1. Thanks also to the anonymous referees.

Conflicts of Interest: The authors declare no conflict of interest. The funders had no role in the design of the study.

References

1. IPCC. IPCC Sixth Assessment Report. Available online: https://www.ipcc.ch/report/ar6/wg1/, (accessed on 13 July 2022).
2. NOAA. Global Monitoring Laboratory. Available online: https://gml.noaa.gov/ccgg/trends/mlo.html, (accessed on 13 July 2022).
3. Jia, Z.; Li, Z. *Carbonate Sedimentary Facies and Sedimentary Environment*; China University of Geosciences Press: Wuhan, China, 1989; pp. 1–6.
4. Wang, S. The most serious ecological and geological environmental problem in southwest China-Karst rock desertification. *Bull Miner. Pet. Geochem* **2003**, *22*, 120–126.
5. Jiang, Z.; Lian, Y.; Qin, X. Rocky desertification in Southwest China: Impacts, causes, and restoration. *Earth Sci. Rev.* **2014**, *132*, 1–12. [CrossRef]
6. Xiong, P.; Yuan, D.; Xie, S. Progress of research on rocky desertification in South China Karst Mountain. *Carsol Sin* **2010**, *29*, 355–356.
7. Oelkers, E.H.; Declercq, J.; Saldi, G.D.; Gislason, S.R.; Schott, J. Olivine dissolution rates: A critical review. *Chem. Geol.* **2018**, *500*, 1–19. [CrossRef]
8. Gaillardet, J.; Galy, A. Himalaya-Carbon Sink or Source. *Science* **2008**, *320*, 1727–1728. [CrossRef] [PubMed]
9. Yuan, D. Progress in the study on "Karst process and carbon cycle". *Adv. Earth Sci.* **1999**, *14*, 425–432.
10. Larson, C. An unsung carbon sink. *Science* **2011**, *334*, 886–887. [CrossRef]
11. Liu, Z. "Method of maximum potential dissolution" to calculate the intensity of karst process and the relevent carbon sink: With discussions on methods of solute load carbonate-rock-tablet test. *Carsol. Sin.* **2011**, *30*, 379–382.
12. Liu, Z.H. New progress and prospects in the study of rock-weathering-related carbon sinks. *Chin. Sci. Bull.* **2012**, *57*, 95–102. [CrossRef]
13. Chen, C.Y.; Liu, Z.H. The role of biological carbon pump in the carbon sink and water environment improvement in karst surface aquatic ecosystems. *Chin. Sci. Bull.* **2017**, *62*, 3440–3450. [CrossRef]
14. Berner, R.A. Atmospheric carbon dioxide levels over Phanerozoic time. *Science* **1990**, *249*, 1382–1386. [CrossRef] [PubMed]
15. Berner, R.A.; Kothavala, Z. GEOCARB III: A revised model of atmospheric CO_2 over Phanerozoic time. *Am. J. Sci.* **2001**, *301*, 182–204. [CrossRef]
16. Curl, R.L. Carbon shifted but not sequestered. *Science* **2012**, *335*, 655. [CrossRef]
17. Yuan, D. Rock desertification in the subtropical karst of south China. *Z. Geomorph. (Suppl.)* **1997**, *108*, 81–90.
18. Cao, J.; Yuan, D.; Pan, G. Sme soil features in karst ecosystem. *Adv. Earth Sci.* **2003**, *18*, 37–44.
19. Legrand, H.E.; Stringfield, V.T. Karst hydrology:A review. *J. Hydrol.* **1973**, *20*, 97–120. [CrossRef]
20. Qin, X. Characteristics and comprehensive treatment strategy of karst drought in Central Guangxi. *J. Guilin Univ. Technol.* **2005**, *25*, 278–283.
21. Yuan, D. Carbon cycle in Earth system and its effects on environment and resources. *Quatern. Sci.* **2001**, *21*, 223–232.
22. Guo, F.; Jiang, G.; Yuan, D. Major ions in typical subterranean rivers and their anthropogenic impacts in southwest karst areas, China. *Environ. Geol.* **2007**, *53*, 533–541. [CrossRef]
23. Song, T.; Peng, W.; Du, H.; Wang, K.; Zeng, F. Occurrence, spatial-temporal dynamics and regulation strategies of karst rocky desertification in southwest China. *Chin. J. Ecol.* **2014**, *34*, 5328–5341.
24. Liu, L.; Zeng, F.; Song, T.; Peng, W.; Wang, K.; Qin, W.; Tan, W. Spatial heterogeneity of soil nutrients in Karst area's Mulun National Nature Reserve. *Chin. J. Appl. Ecol.* **2010**, *21*, 1667–1673.
25. Dong, L.; He, T.; Liu, Y.; Shu, Y.; Luo, H.; Liu, F. Changes of soil physical- chemical properties derived from different parent materials/rocks in karst mountain. *Chin. J. Soil Sci.* **2008**, *39*, 471–474.
26. Ji, F.; Li, N.; Deng, X. Calcium contents and high calcium adaptation of plants in karst area of China. *Chin. J. Plant Ecol.* **2009**, *33*, 926–935.
27. Xiong, D.; Cai, H.; Zhang, R.; Li, C.; QIan, X. Distribution of soil medium and micro-elements in Fujian tobacco-growing soils. *Chin. J. Eco Agric.* **2007**, *15*, 36–38.
28. Li, Z.; Zou, B.; Cao, Y.; Ren, H.; Liu, J. nutrient characteristics of soils in typical degraded hilly land in Southern China. *Acta. Ecol. Sin.* **2003**, *23*, 1648–1656.
29. Paramasivam, S.; Alva, A.K. Nitrogen recovery from controlled-release fertilizers under intermittent leaching and dry cycles. *Soil Sci.* **1997**, *162*, 447–453. [CrossRef]
30. Wei, X.; Shao, M. The distribution of soil nutrients on sloping land in the gully regiion watersheds of the Loess Plateau. *Acta. Ecol. Sin.* **2007**, *27*, 603–613.
31. Liu, C. *Biogeochemical Processes and Cycling of Nutrients in the Earth's Surface: Cycling of Nutrients in Soil-Plant Systems of Karstic Environments, Southwest China*; Science Press of China: Beijing, China, 2009; pp. 308–353, 401–443.
32. National Soil Census Office of China. *Soil in China*; China Agriculture Press: Beijing, China, 1998; pp. 843–984.

33. Jiang, D.; Cheng, J. Changes of pH and available pool of B, Cu, Zn, Mn in surface rice soils in Yixing, Jiangsu province over the last decade. *J. Nanjing Agric. Univ.* **1997**, *20*, 111–113.
34. Wu, Y.Y.; Xing, D.K. Effect of bicarbonate treatment on photosynthetic assimilation of inorganic carbon in two plant species of *Moraceae*. *Photosynth.* **2012**, *50*, 587–594. [CrossRef]
35. Wu, Y.; Li, H.; Xie, T. *Biogeochemical Action of Microalgal Carbonic Anhydrase*; Science Press of China: Beijing, China, 2015; pp. 75–110.
36. Hang, H.T.; Wu, Y.Y. Quantification of photosynthetic inorganic carbon utilisation via a bidirectional stable carbon isotope tracer. *Acta. Geochim.* **2016**, *35*, 130–137. [CrossRef]
37. Rao, S.; Wu, Y.Y. Root-derived bicarbonate assimilation in response to variable water deficit in *Camptotheca acuminate* seedlings. *Photosyn. Res.* **2017**, *134*, 59–70. [CrossRef] [PubMed]
38. Wang, R.; Wu, Y.; Xing, D.; Hang, H.; Xie, X.; Yang, X.; Zhang, K.; Rao, S. Biomass production of three biofuel energy plants' use of a new carbon resource by carbonic anhydrase in simulated karst soils: Mechanism and capacity. *Energies* **2017**, *10*, 1370. [CrossRef]
39. Xie, T.; Wu, Y. The biokarst system and its carbon sinks in response to pH changes: A simulation experiment with microalgae. *Geochem. Geophys. Geosyst.* **2017**, *18*, 827–843. [CrossRef]
40. Wu, Y.; Xing, D.; Hang, H.; Zhao, K. *Principles and Techniques of Determination on Plants' Adaptation to Karst Environment*; Science Press of China: Beijing, China, 2018; pp. 1–188.
41. Fang, L.; Wu, Y.Y. Bicarbonate uptake experiment show potential karst carbon sinks transformation into carbon sequestration by terrestrial higher plants. *J. Plant Interact.* **2022**, *17*, 419–426. [CrossRef]
42. Wu, Y. Combined effect of bicarbonate and water in photosynthetic oxygen evolution and its implication for carbon neutrality. *Sci. Bull.* **2022**. submitted and revised.
43. He, S.; Yu, S.; Pu, J.; Yuan, Y.; Zhang, C. Dynamics in Riverine Inorganic and Organic Carbon Based on Carbonate Weathering Coupled with Aquatic Photosynthesis in a Karst Catchment, Southwest China. *Water Res.* **2021**, *189*, 116658.
44. Yang, R.; Sun, H.; Chen, B.; Yang, M.; Zeng, Q.; Zeng, C.; Huang, J.; Luo, H.; Lin, D. Temporal variations in riverine hydrochemistry and estimation of the carbon sink produced by coupled carbonate weathering with aquatic photosynthesis on land: An example from the Xijiang River, a large subtropical karst-dominated river in China. *Environ. Sci. Pollut. Res.* **2020**, *27*, 13142–13154. [CrossRef]
45. Cao, J.H.; Wu, X.; Huang, F.; Hu, B.; Groves, C.; Yang, H.; Zhang, C.L. Global significance of the carbon cycle in the karst dynamic system: Evidence from geological and ecological processes. *China Geol.* **2018**, *1*, 17–27. [CrossRef]
46. Berner, R.A. The carbon cycle and carbon dioxide over Phanerozoic time: The role of land plants. *Philos. Trans. R. Soc. B* **1998**, *353*, 75–82. [CrossRef]
47. Moulton, K.L.; Berner, R.A. Quantification of the effect of plants on weathering: Studies in Iceland. *Geology* **1998**, *26*, 895–898. [CrossRef]
48. Knoll, A.H.; Nowak, M.A. The timetable of evolution. *Sci. Adv.* **2017**, *3*, e1603076. [CrossRef] [PubMed]
49. Hart, M.H. The evolution of the atmosphere of the Earth. *Icarus* **1978**, *33*, 23–39. [CrossRef]
50. Des Marais, D.J. When did photosynthesis emerge on Earth? *Science* **2000**, *289*, 1703–1705. [CrossRef]
51. Dismukes, G.C.; Klimov, V.V.; Baranov, S.V.; Kozlov, Y.N.; DasGupta, J.; Tyryshkin, A. The origin of atmospheric oxygen on Earth: The innovation of oxygenic photosynthesis. *Proc. Natl. Acad. Sci. USA* **2001**, *98*, 2170–2175. [CrossRef] [PubMed]
52. Pagani, M.; Caldeira, K.; Berner, R.A.; Beerling, D.J. The role of terrestrial plants in limiting atmospheric CO_2 decline over the past 24 million years. *Nature* **2009**, *460*, 85–88. [CrossRef] [PubMed]
53. Kasting, J.F. Earth's early atmosphere. *Science* **1993**, *259*, 920–926. [CrossRef]
54. Halevy, I.; Bachan, A. The geologic history of seawater pH. *Science* **2017**, *355*, 1069–1071. [CrossRef]
55. Teng, F.Z.; Ma, L. Deciphering isotope signatures of Earth Surface and Critical Zone processes. *Chem. Geol.* **2016**, *445*, 1–3. [CrossRef]
56. Schwender, J.; Goffman, F.; Ohlrogge, J.B.; Shachar-Hill, Y. Rubisco without the Calvin cycle improves the carbon efficiency of developing green seeds. *Nature* **2004**, *432*, 779–782. [CrossRef]
57. Tcherkez, G.; Mahe, A.; Gauthier, P.; Mauve, C.; Gout, E.; Bligny, R.; Cornic, G.; Hodges, M. In folio respiratory fluxomics revealed by ^{13}C isotopic labeling and H/D isotope effects highlight the noncyclic nature of the tricarboxylic acid "Cycle" in illuminated leaves. *Plant Physiol.* **2009**, *151*, 620–630. [CrossRef]
58. Lin, G. Stable isotope ecology: A new branch of ecology resulted from technology advances. *Chin. J. Plant Ecol.* **2010**, *34*, 119–122.
59. Nichols, J.; Booth, R.K.; Jackson, S.T.; Pendall, E.G.; Huang, Y.S. Differential hydrogen isotopic ratios of *Sphagnum* and vascular plant biomarkers in ombrotrophic peatlands as a quantitative proxy for precipitation-evaporation balance. *Geochim. Cosmochim. Acta* **2010**, *74*, 1407–1416. [CrossRef]
60. Broeckx, L.S.; Fichot, R.; Verlinden, M.S.; Ceulemans, R. Seasonal variations in photosynthesis, intrinsic water-use efficiency and stable isotope composition of poplar leaves in a short-rotation plantation. *Tree Physiol.* **2014**, *34*, 701–715. [CrossRef] [PubMed]
61. Xie, T.; Wu, Y. The role of microalgae and their carbonic anhydrase on the biological dissolution of limestone. *Environ. Earth Sci.* **2014**, *71*, 5231–5239. [CrossRef]
62. Hang, H. Expression Encoding Carbonic Anhydrase Gene and Inorganic Carbon Utilization of the Two Plants Species under Karst Environment. Ph.D. Dissertation, The University of Chinese Academy of Sciences, Beijing, China, 2015.

63. Yan, W.; Zeng, C.; Xiao, S.; Lan, J.; Dai, L.; Tai, Z.; He, J.; He, C.; Di, Y. Dissolution rate and karst carbon sink of different land use in typical dolomite watershed with humid subtropical weather. *Earth Environ.* **2021**, *49*, 529–538.
64. Zeng, C.; Zhao, M.; Yang, R.; Liu, Z. Comparison of karst processes-related carbon sink intensity calculated by carbonate rock tablet test and solute load method: A case study in the Chenqi karst spring system. *Hydrogeo Eng. Geol.* **2014**, *41*, 106–111.
65. Lan, J.C.; Fu, W.L.; Peng, J.T.; Zhou, X.P.; Xiao, S.Z.; Yuan, B. Dissolution rate under soil in karst areas and the influencing factors of different land use patterns. *Acta Ecol. Sin.* **2013**, *33*, 3205–3212.
66. Zhang, C. Carbonate rock dissolution rates in different land uses and their carbon sink effect. *Chin. Sci. Bull.* **2011**, *56*, 3759–3765. [CrossRef]
67. Zeng, C.; Liu, Z.; Zhao, M.; Yang, R. Hydrologically-driven variations in the karst-related carbon sink fluxes: Insights from high-resolution monitoring of three karst catchments in Southwest China. *J. Hydrol.* **2016**, *533*, 74–90. [CrossRef]
68. Zeng, C.; He, C.; Xiao, S.; Liu, Z.; Chen, W.; He, J. Karst related inorganic carbon sink flux in a typical humid subtropical dolomite basin. *Earth Sci. Front.* **2022**, *29*, 179–188.
69. Li, S.; Liu, C.; Li, J.; Lang, Y.; Ding, H.; Li, L. Geochemistry of dissolved inorganic carbon and carbonate weathering in a small typical karstic catchment of Southwest China: Isotopic and chemical constraints. *Chem. Geol.* **2010**, *277*, 301–309. [CrossRef]
70. Yu, W.; Dong, D.; Ni, J. Comparison of biomass and net primary productivity of Karst and non-karst forests in mountainous area, Southwestern China. *J. Subtrop. Resour. Environ.* **2010**, *5*, 25–30.
71. Wu, Y.; Rao, S.; Wu, Y.; Fang, L.; Su, Y.; Li, H.; Wang, R.; Wang, S.; Liu, C. *A Method for Obtaining the Share of Bicarbonate Utilization by Plants in Natural Habitats*; ZL2018103132903, Beijing; CN108319820B; State Intellectual Property Office of China: Beijing, China, 2018.
72. Xia, H. Biomass and net primary production in different successional stages of karst vegetation in Maolan, SW China, Guizhou. *For. Sci. Technol.* **2010**, *38*, 1–7.
73. Veitch, F.P.; Blankenship, L.C. Carbonic anhydrase in bacteria. *Nature* **1963**, *197*, 76–77. [CrossRef] [PubMed]
74. Badger, M.R.; Price, G.D. The role of carbonic anhydrase in photosynthesis. *Annu. Rev. Plant Biol.* **1994**, *45*, 369–392. [CrossRef]
75. Smith, K.S.; Ferry, J.G. Prokaryotic carbonic anhydrases. *FEMS Microbiol. Rev.* **2000**, *24*, 335–366. [CrossRef] [PubMed]
76. Gilmour, K.M.; Perry, S.F. Carbonic anhydrase and acid-base regulation in fish. *J. Exp. Biol.* **2009**, *212*, 1647–1661. [CrossRef] [PubMed]
77. Price, G.D.; Long, B.M.; Förster, B. DABs accumulate bicarbonate. *Nat. Microbiol.* **2019**, *4*, 2029–2030. [CrossRef]
78. Ivanov, B.N.; Ignatova, L.K.; Romanova, A.K. Diversity in forms and functions of carbonic anhydrase in terrestrial higher plants. *Russ. J. Plant Physl.* **2007**, *54*, 143–162. [CrossRef]
79. Sun, W.; Wu, Y.; Wen, X.; Xiong, S.; He, H.; Wang, Y.; Lu, G. Different mechanisms of photosynthetic response to drought stress in tomato and violet orychophragmus. *Photosynthetica* **2016**, *54*, 226–233. [CrossRef]
80. DiMario, R.J.; Machingura, M.C.; Waldrop, G.L.; Moroney, J.V. The many types of carbonic anhydrases in photosynthetic organisms. *Plant Sci.* **2018**, *268*, 11–17. [CrossRef]
81. Hang, H.; Wu, Y. Effect of bicarbonate stress on carbonic anhydrase gene expressions from *Orychophragmus violaceus* and *Brassica juncea* seedlings. *Pol. J. Environ. Stud.* **2019**, *28*, 1135–1143. [CrossRef]
82. Liu, Z.; Dreybrod, W. Dissolution kinetics of calcium carbonate minerals in H_2O–CO_2 solutions in turbulent flow: The role of the diffusion boundary layer and the slow reaction $H_2O + CO_2 \rightarrow H^+ + HCO_3^-$. *Geochim. Cosmochim. Acta* **1997**, *61*, 2879–2889. [CrossRef]
83. Li, W.; Yu, L.J.; Wu, Y.; Jia, L.P.; Yuan, D.X. Enhancement of Ca^{2+} release from limestone by microbial extracellular carbonic anhydrase. *Bioresour. Technol.* **2007**, *98*, 950–953. [CrossRef] [PubMed]
84. Liu, Z. Role of carbonic anhydrase as an activator in carbonate rock dissolution and its implication for atmospheric CO_2 sink. *Acta Geol. Sin. (Engl. Ed.)* **2001**, *75*, 275–278.
85. Papamichael, E.M.; Economou, E.D.; Vaimakis, T.C. Dissolution of the carbonate minerals of phosphate ores: Catalysis by carbonic anhydrase II, from bovine erythrocytes, in acid solutions. *J. Colloid Interf. Sci.* **2002**, *251*, 143–150. [CrossRef] [PubMed]
86. Seibt, U.; Wingate, L.; Lloyd, J.; Berry, J.A. Diurnally variable $\Delta^{18}O$ signatures of soil CO_2 fluxes indicate carbonic anhydrase activity in a forest soil. *J. Geophy. Res. Biogeo.* **2006**, *111*, G04005.
87. Wingate, L.; Seibt, U.; Maseyk, K.; Ogee, J.; Almeida, P.; Yakir, D.; Pereira, J.; Mencuccini, M. Evaporation and carbonic anhydrase activity recorded in oxygen isotope signatures of net CO_2 fluxes from a Mediterranean soil. *Glob. Change Biol.* **2008**, *14*, 2178–2193. [CrossRef]
88. Von Sperber, C.; Weiler, M.; Brüggemann, N. The effect of soil moisture, soil particle size, litter layer and carbonic anhydrase on the oxygen isotopic composition of soil-released CO_2. *Eur. J. Soil Sci.* **2015**, *66*, 566–576. [CrossRef]
89. Hu, H.; Boisson-Dernier, A.; Israelsson-Nordström, M.; Böhmer, M.; Xue, S.; Ries, A.; Godoski, J.; Kuhn, J.M.; Schroeder, J.I. Carbonic anhydrases are upstream regulators of CO_2-controlled stomatal movements in guard cells. *Nat. Cell Biol.* **2010**, *12*, 87–93. [CrossRef]
90. Hu, H.; Rappel, W.J.; Occhipinti, R.; Ries, A.; Böhmer, M.; You, L.; Xiao, C.; Engineer, C.B.; Boron, W.F.; Schroeder, J.I. Distinct cellular locations of carbonic anhydrases mediate carbon dioxide control of stomatal movements. *Plant Physiol.* **2015**, *169*, 1168–1178. [CrossRef] [PubMed]

91. Wu, Y.Y.; Liu, C.Q.; Li, P.P.; Wang, J.Z.; Xing, D.; Wang, B.L. Photosynthetic characteristics involved in adaptability to Karst soil and alien invasion of paper mulberry (*Broussonetia papyrifera* (L.) Vent.) in comparison with mulberry (*Morus alba* L.). *Photosynthetica* **2009**, *47*, 155–160. [CrossRef]
92. Nathan, V.K.; Ammini, P. Carbon dioxide sequestering ability of bacterial carbonic anhydrase in a mangrove soil microcosm and its bio-mineralization properties. *Water Air Soil Pollut.* **2019**, *230*, 192. [CrossRef]
93. Wu, Y.; Liu, C.; Wang, S. *Adaptability to Karst of Orychophragmus violaceus*; Guizhou Science and Technology Press: Guiyang, China, 2014; pp. 1–153.
94. Xia, A.; Wu, Y. Joint interactions of carbon and nitrogen metabolism dominated by bicarbonate and nitrogen in *Orychophragmus violaceus* and *Brassica napus* under simulated karst habitats. *BMC Plant Biol.* **2022**, *22*, 264. [CrossRef]
95. Wu, Y. Strategies to increase carbon fixation and sequestration by Karst-adaptable plants. *Carsol. Sin.* **2011**, *30*, 461–465.